Research article

Template-free microwave-assisted hydrothermal synthesis of manganese zinc ferrite as a nanofertilizer for squash plant (*Cucurbita pepo L*)

Ahmed Shebl [a,*], A.A. Hassan [a], Dina M. Salama [b], Mahmoud E. Abd El-Aziz [c], Mohamed S.A. Abd Elwahed [d]

[a] Chemistry Department, Faculty of Science, Ain Shams University, Abbassia, Cairo, Egypt
[b] Vegetable Research Department, National Research Centre, Giza, Egypt
[c] Polymers & Pigments Department, National Research Centre, Giza, Egypt
[d] Botany Department, National Research Centre, Giza, Egypt

ARTICLE INFO

ABSTRACT

Manganese, zinc, and iron are the most essential micronutrients required for plant growth and applied as foliar fertilizers. Herein, a simple template-free microwave-assisted hydrothermal green synthesis technique was adapted to produce manganese zinc ferrite nanoparticles ($Mn_{0.5}Zn_{0.5}Fe_2O_4$ NPs) at different temperatures (100, 120, 140, 160 and 180 °C). The prepared nanomaterials were employed at different concentrations (0, 10, 20, and 30 ppm) as foliar nanofertilizers during the squash (*Cucurbita pepo* L) planting process. X-ray diffraction patterns of the prepared nanomaterials confirmed successful production of the nanoferrite material. The prepared nano-fertilizers showed type IV adsorption isotherm characteristic for mesoporous materials. FE-SEM and HR-TEM imaging showed that the nanoparticles were cubic shaped and increased in particle size with the increase in microwave temperature during production. The impact of application of the synthesized ferrite nanoparticles on vegetative growth, proximate analysis, minerals content and the yield of squash plant was investigated for two consecutive successful planting seasons. The nanoferrite synthesized at 160 °C and applied to the growing plants at a concentration of 10 ppm gave the highest increase in % yield (49.3 and 52.9%) compared to the untreated squash for the two consecutive seasons, whereas the maximum organic matter content (73.0 and 72.5%) and total energy (260 and 258.3 kcal/g) in squash leaves were obtained in plants treated with 30 ppm ferrite nanoparticles synthesized at 180 °C. On the other hand, the maximum organic matter content (76.6 and 76.3%) and total energy (253.6 and 250.3 kcal/g) in squash fruits were attained with plants supplied by 20 ppm ferrite nano-particles synthesized at 160 °C. These results indicate that the simple template-free microwave-assisted hydro-thermal green synthesis technique for the production of manganese zinc ferrite nanoparticles yields nanoparticles appropriate for use as fertilizer for *Cucurbita pepo* L.

1. Introduction

Globally, agricultural production suffers from the poor efficacy of currently available fertilizers. The low thermal stability, high solubility and small molecular weight of traditional fertilizers increases the tendency of these materials to transfer to the air or the surrounding water through volatilization, runoff and leaching, thereby causing intense environmental pollution [1, 2, 3]. Recently, nanofertilizers have been used as effective fertilizers during the planting process due to their higher bioavailability and minimal environmental impact via limiting losses of such nutrients to the surrounding environment [4, 5, 6]. These

nanofertilizers can be applied as encapsulated nanomaterials [7], impeded inside a polymeric membrane [8], or delivered as nanoparticles [9, 10].

Spinel ferrites are widely used magnetic materials [11, 12, 13], with their thermal and chemical stability rendering them appropriate materials in a range of applications including gas sensing [14], manufacture of magnetic recording devices [13], and as carriers for targeted drug delivery [15]. Nonetheless, to date, their application in agricultural production has been limited. To the best of our knowledge, this is the first study using such materials as nanofertilizers.

* Corresponding author.
  E-mail address: a_ahmed@sci.asu.edu.eg (A. Shebl).
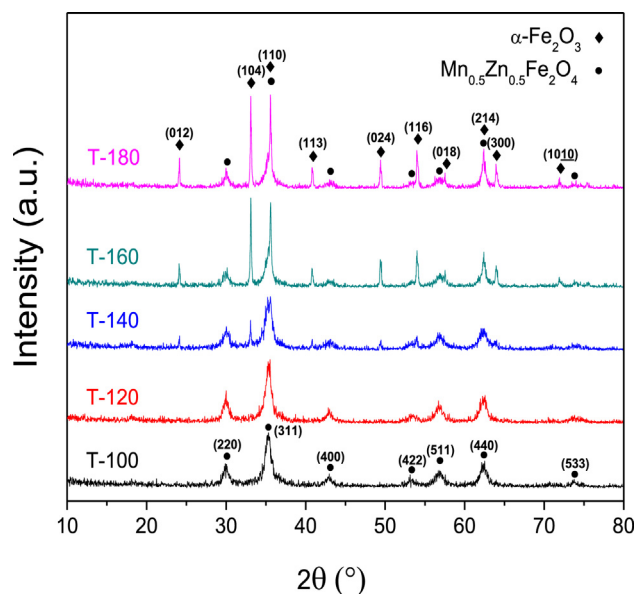
Figure 1. XRD patterns of the prepared ferrite nanofertilizer samples.

Squash (*Cucurbita pepo* L.) is one of the most essential summer crops that belongs to the *Cucurbitaceae* family [16], and is important not only due to its use as human food but also as a medicinal plant. In Egypt, it is an annual crop, grown for its edible fruits which are cooked and processed. Many factors affect the quantity and quality of squash harvest, the most important being fertilization [1, 8, 17]. Recently, nanofertilizers had been utilized instead of traditional fertilizers [5, 18, 19] as nanoparticles (NPs) can interact with plants producing many morphological and physiological changes, leading to higher quality harvests [2, 20]. The efficacy of such NPs is strongly correlated to their chemical composition, size, surface covering, reactivity, as well as the amount applied [21].

Micronutrients, such as iron, manganese, zinc, copper, boron and molybdenum, are essential elements required in small amounts for plant growth [22], which are applied as foliar fertilizers to improve the agro-morphological criteria and the yield [23]. The foliar application of micronutrients is a valuable practice due to the small quantity required, does not directly contact the soil, and avoid losses during fixation, consequently, is more effective than soil application [24, 25]. Zinc has an essential function in carbohydrate and protein metabolism, as well as controlling plant growth hormone [26, 27]. It is also necessary for the synthesis of tryptophan, a precursor of indole acetic acid [28]. Manganese is an essential micronutrient for plant nutrition, which functions as a catalyst in the oxygen-evolving complex of the photosystem, respiration and nitrogen assimilation [29]. It is required by plants in the second greatest quantity compared to iron, so competes with the micronutrients (Fe, Zn, Cu, Mg and Ca) for uptake by the plant [30]. Iron is constitutive for many enzymes and pigments, facilitating the reduction of nitrate and sulfate, as well as the production of energy in the plant. Although iron is not used in the synthesis of chlorophyll, it is necessary for its formation [31].

Sheykhbaglou *et al.* [32] found that mineral elements (Fe, Mg, Ca and P), chlorophyll content, as well as the lipid and protein levels were raised by increasing the content of ferrous oxide NPs in soybean plants via foliar application. However, it has been reported that the impact of NPs on plants depends on their composition, concentration, and size, as well as the physical and chemical properties of NPs and plant species [18, 21]. Amorós Ortiz-Villajos *et al.* [33] reported that the minerals such as Fe, Zn, Cu, and Ni accumulated in roots, Mg and Mn in leaves, S, Ca, and Mo in leaves and roots, while K accumulates in leaves, roots, and stems. In addition, there are favourable correlations between the changes in the content of the mineral pairs, Fe–Mn, K–S, Fe–Ni, Cu–Mg, Mn–Ni, S–Mo, Mn–Ca, and Mn–Mg, throughout the reproduction of rice in the organs above ground and the concentration of Fe–Mn and K–S in roots.

In the present study, microwave-assisted hydrothermal synthesis technique [34, 35, 36] was used to prepare manganese zinc ferrite nanoparticles ($Mn_{0.5}Zn_{0.5}Fe_2O_4$ NPs). This method is a facile, fast, secure, controllable and energy-saving process [37, 38], which can dramatically decrease the synthesis process from days and hours to a few minutes. It also provides an effective way to control particle size distribution and macroscopic morphology during the synthesis process [39, 40]. The impact of the application of the synthesised ferrite nanoparticles on vegetative growth, proximate analysis, mineral content and the yield of squash plant was investigated for two consecutive successful planting seasons.

2. Materials and methods

2.1. Materials

All chemicals were analytical grade and used without any further purification: $Fe(NO_3)_3.9H_2O$ was 99% purity and purchased from Winlab (UK); $Mn(NO_3)_2.4H_2O$ (purity $\geq 97\%$) was from Sigma-Aldrich; $Zn(NO_3)_2.6H_2O$, 96% pure was obtained from S.D. fine-chem Ltd (India); NaOH flakes were GPR 99% grade and purchased from Alpha chemicals, Egypt.

2.2. Preparation of manganese zinc ferrite nanoparticles ($Mn_{0.5}Zn_{0.5}Fe_2O_4$ NPs)

The ferrite nanofertilizer samples were prepared using a green microwave-assisted hydrothermal method. The appropriate amounts of $Zn(NO_3)_2.6H_2O$, $Mn(NO_3)_2.4H_2O$, and $Fe(NO_3)_3.9H_2O$ were dissolved in distilled water in a ratio of 0.5:0.5:2 for the formation of $Mn_{0.5}Zn_{0.5}Fe_2O_4$. The pH was adjusted to 10 by NaOH solution. The slurry was then transferred to 100 mL Teflon autoclave vessel and microwaved in a 750 W advanced microwave synthesis lab station (Milestone MicroSYNTH). The microwave was adjusted to reach the chosen temperature in 3 min, then the reaction vessel was maintained at this temperature for 10 min. Five ferrite samples were prepared at different holding temperatures, 100, 120, 140, 160, and 180 °C to obtain ferrite nanofertilizer samples T-100, T-120, T140, T-160 and T-180, respectively. The obtained ferrite nanofertilizer was then washed three times with distilled water, dried at 100 °C for 6 h, ground, and stored in a desiccator for further characterization studies.

2.3. Characterization of ferrite nanofertilizer

The prepared ferrite nanofertilizer samples were characterized via X-ray diffraction (XRD) using a PHILIPS® X'Pert diffractometer with the Bragg-Brentano geometry and copper tube at operating voltage of 40 kV and current of 30 mA. For the quantification of crystalline phases in the prepared samples, the XRD profile was refined using the Rietveld method which employs Materials Analysis Using Diffraction (MAUD) software.

The surface characteristics of the prepared samples were investigated using fully automated BELSORP-mini II to obtain the adsorption-desorption isotherms of N_2 at 77 K. The Barrett-Joyner-Halenda (BJH) method was utilized for the calculation of pore size distribution.

A morphological study of the prepared samples, as well as particles shape observation and quantitative measurement of their sizes were performed via Field Emission Scanning Electron Microscopy (FE-SEM) using a Quanta 250 and high-resolution field emission gun (HRFEG), and High-Resolution Transmission Electron Microscope (HR-TEM; JEM2100).

2.4. Plant material vegetal

Squash seeds (cv. Eskandarani F1) were purchased from the Agricultural Research Centre (Egypt) and cultivated in clay soil at rate of one seed per hill and 50 cm between hills on one side of a ridge and 70 cm between the ridges on the 1st of March in two seasons (2017 & 2018) in Shebin El-Kom, El-Monifia governorate, Egypt.
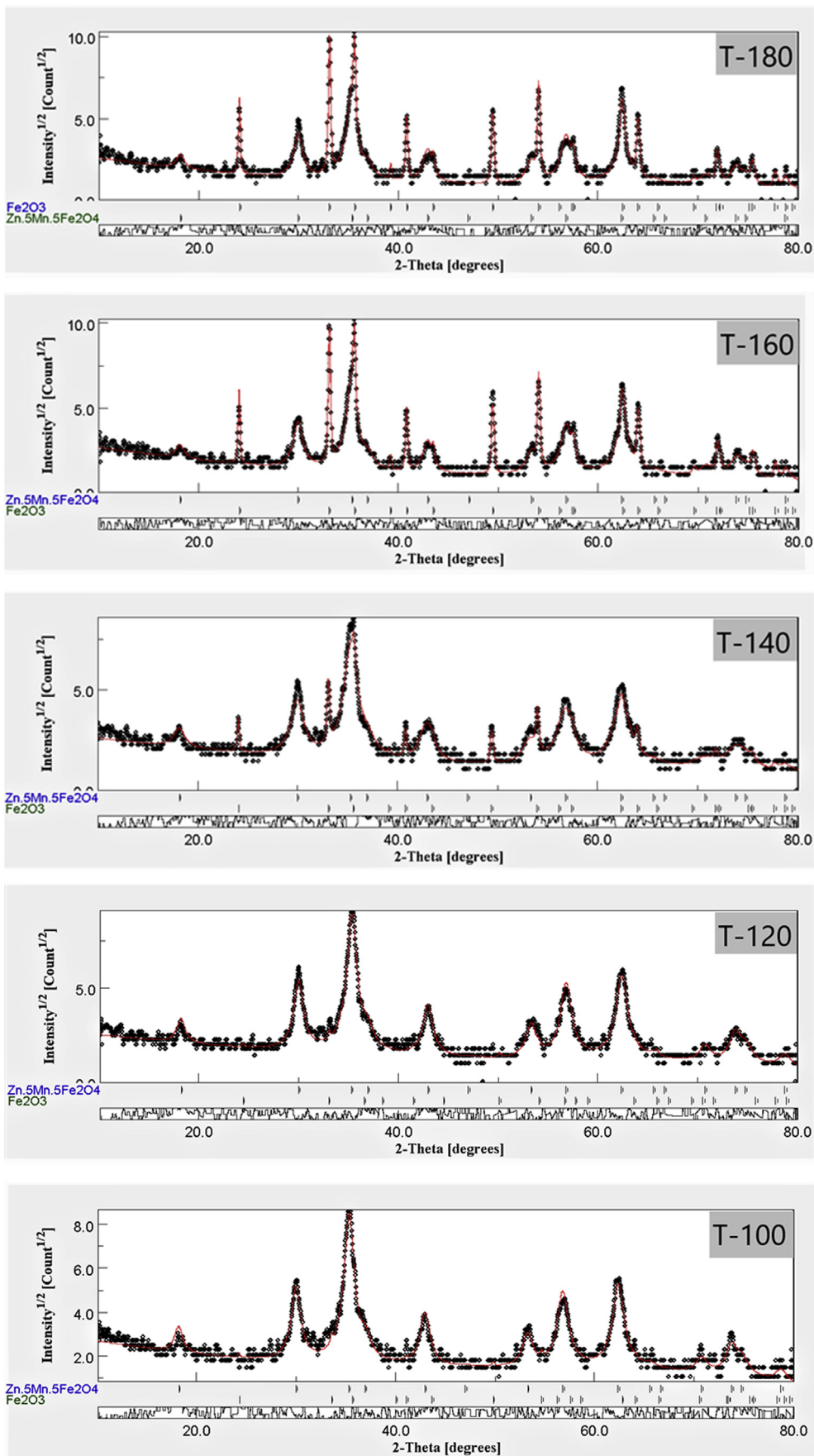
Figure 2. Maud refinement of the XRD data of ferrite nanofertilizer samples.

Table 1. The proportion percentage of $Mn_{0.5}Zn_{0.5}Fe_2O_4$ and Fe_2O_3 in each sample obtained from the refined XRD data MAUD software.

Sample	$Mn_{0.5}Zn_{0.5}Fe_2O_4$ (%)	Fe_2O_3 (%)
T-100	99.0	1.0
T-120	99.0	1.0
T-140	87.7	12.3
T-160	59.5	40.5
T-180	56.8	43.2

Table 2. The surface characteristics of the prepared ferrite nanofertilizer samples.

Ferrite nanofertilizer Samples	Surface area ($m^2 g^{-1}$)	Mean pore radius (nm)	Total pore volume ($cm^3 g^{-1}$)
T-100	162.44	2.69	0.2187
T-120	135.62	3.15	0.2140
T-140	130.02	2.96	0.1927
T-160	69.98	4.34	0.1521
T-180	65.35	4.79	0.1567

2.5. Experimental treatments

The squash plants were sprayed with different concentrations (0, 10, 20 and 30 ppm) of ferrite nanofertilizer samples prepared at different temperatures (T-100, T-120, T-140, T-160 and T-180). The experimental design was a split plot design, with the main plot including the various ferrite nanofertilizer samples prepared at different temperatures and the various concentrations arranged randomly within the sub-plots. Squash plants were sprayed with the ferrite nanofertiliser 20 days after sowing, with the fertilization, weed control and disease resistance, and irrigation of squash plants executed according to the recommendations of the Egyptian Ministry of Agriculture [41].

2.6. Plant growth analysis

Five squash plants were randomly taken from each experimental plot 35 days after seeding to measure the following vegetative growth parameters: plant length, number of leaves per plant, leaf area/plant, and the fresh and dry weight of the whole plant. At harvest (40 days after sowing), the fruits of the squash plants were collected for a month to determine the diameter and length of fruit, plus the yield/plant (kg/plant) and the yield (t/ha).

2.7. Chemical analysis

The squash samples (leaves and fruits) were dried until constant weight at 60 °C in an oven for proximate and mineral analyses.

2.7.1. Proximate analysis

The content of organic matter, protein, fiber, lipids, carbohydrates and ash were calculated according to AOAC [42, 43]. The total energy was calculated by the Atwater factor method [(9 x fat) + (4 x carbohydrate) + (4 x protein)] according to Nwabueze [44].
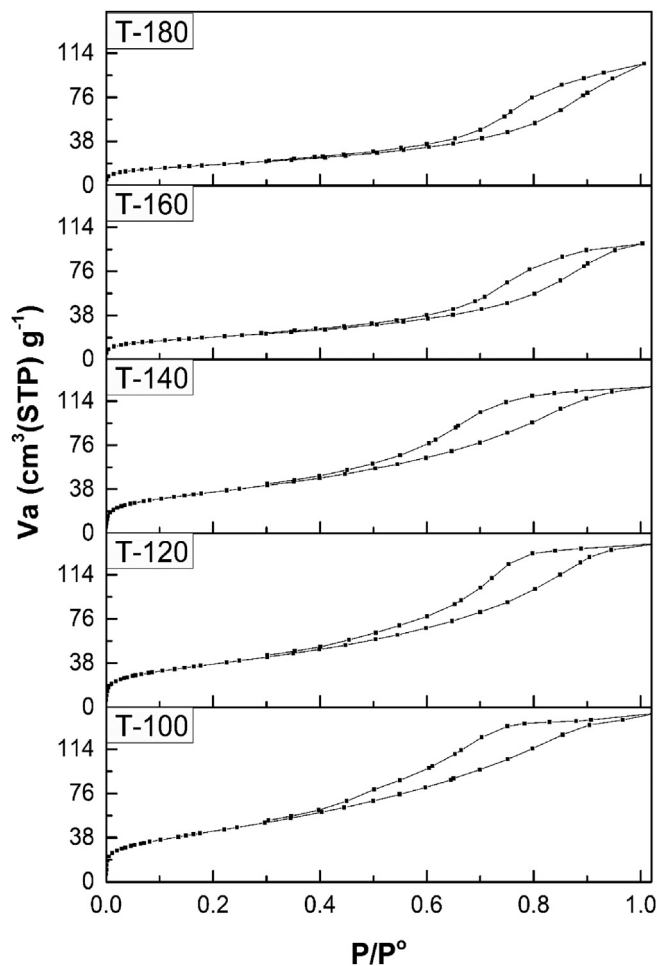
Figure 3. Adsorption-desorption isotherms of N_2 at 77 K on ferrite nanofertilizer samples.
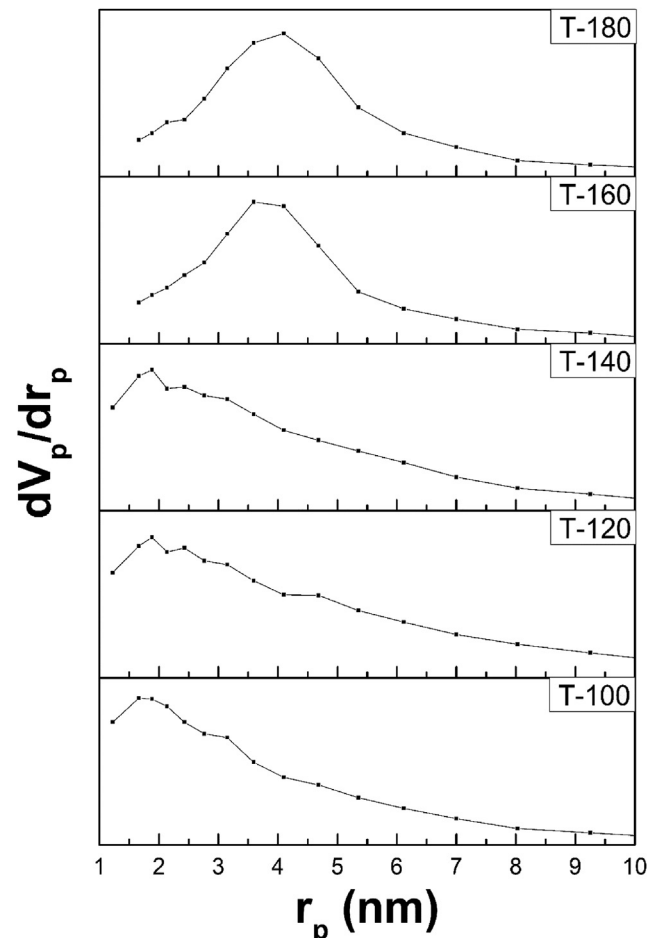
Figure 4. Pore size distribution curves for ferrite nanofertilizer samples.

2.7.2. Minerals determination

Plant samples were ground and digested with H_2SO_4–H_2O_2. The content of the minerals in the digested solution was determined according to the standard methods of the AOAC [42]. The phosphorus and potassium content (%) was determined by a spectrophotometer, while the concentration of zinc, copper, iron and manganese (ppm) was determined by atomic absorption. The nitrogen percentage was determined by the Kjeldahl method [45].

2.8. Statistical analysis

The experimental data were subjected to statistical analysis of variance (ANOVA) and analyzed for significant differences using the LSD test at 5% level according to the procedures described by Kobata *et al.* [46].

3. Results and discussion

3.1. Characterization of the ferrite nanofertilizers

3.1.1. Phase and crystal parameters

XRD analysis showed that all samples had diffraction peaks at 2θ values of 30°, 35.3°, 42.9°, 53.1°, 56.8°, 62.4° and 73.7°, which were identified as the (2 2 0), (3 1 1), (4 0 0), (4 2 2), (5 1 1), (4 4 0) and (5 3 3) lattice planes of the cubic spinel crystal structure of $Mn_{0.5}Zn_{0.5}Fe_2O_4$, respectively (Figure 1) [35,47]. In addition, samples prepared at the higher microwave holding temperature, T-140, T-160, and T-180, showed additional XRD patterns at 2θ values of 24.1°, 33°, 35.5°, 40.8°, 49.4°, 53.9°, 57.5°, 62.4°, 63.9° and 71.9°, which were interpreted as α-Fe_2O_3 characteristic for (0 1 2), (1 0 4), (1 1 0), (1 1 3), (0 2 4), (1 1 6), (0 1 8), (2 1 4), (3 0 0) and (1 0 <u>10</u>) crystal planes, respectively [48, 49].
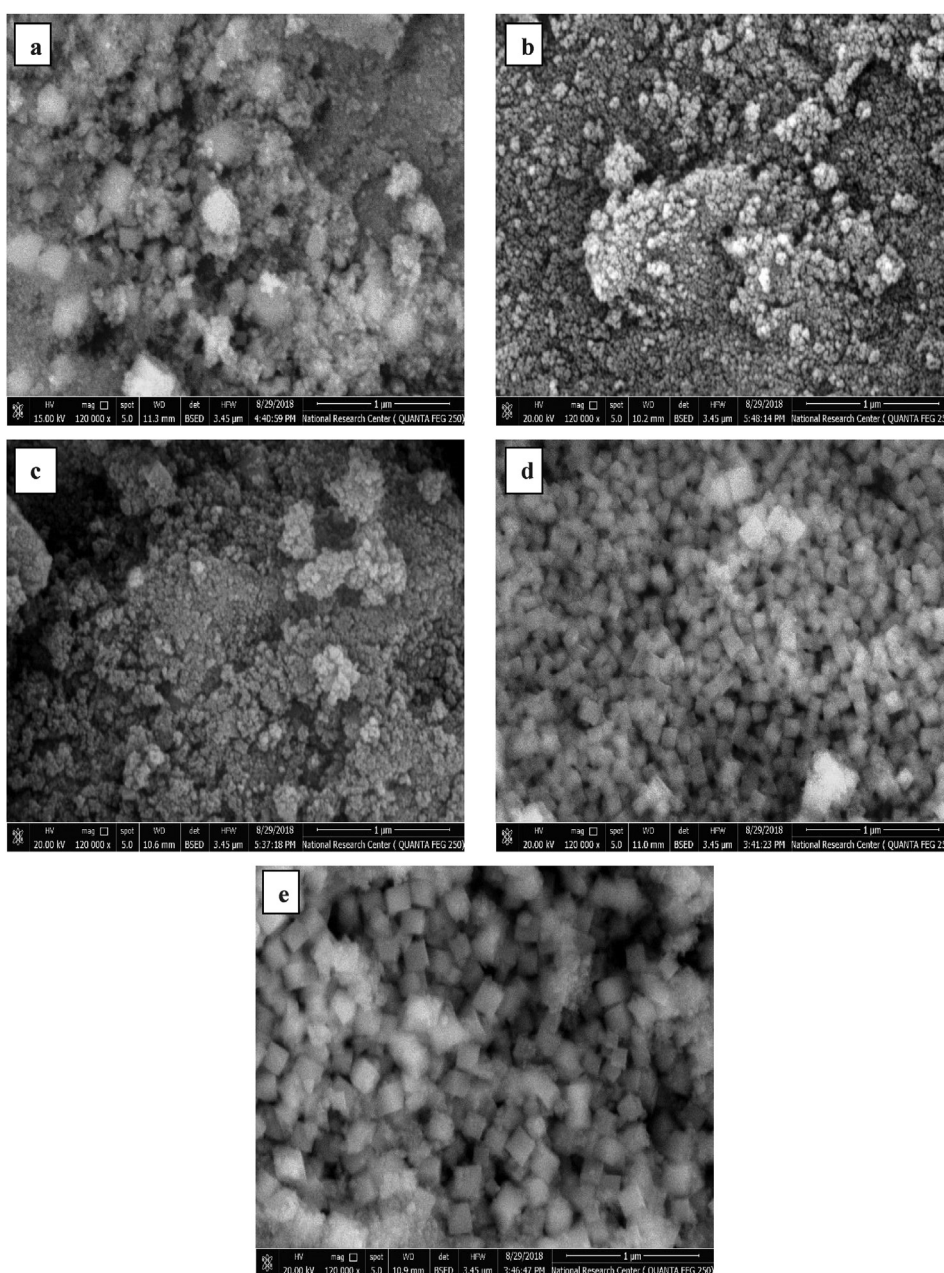
Figure 5. FE-SEM images of ferrite nanofertilizer samples (a) T-100, (b) T-120, (c) T-140, (d) T-160, and (e) T-180.
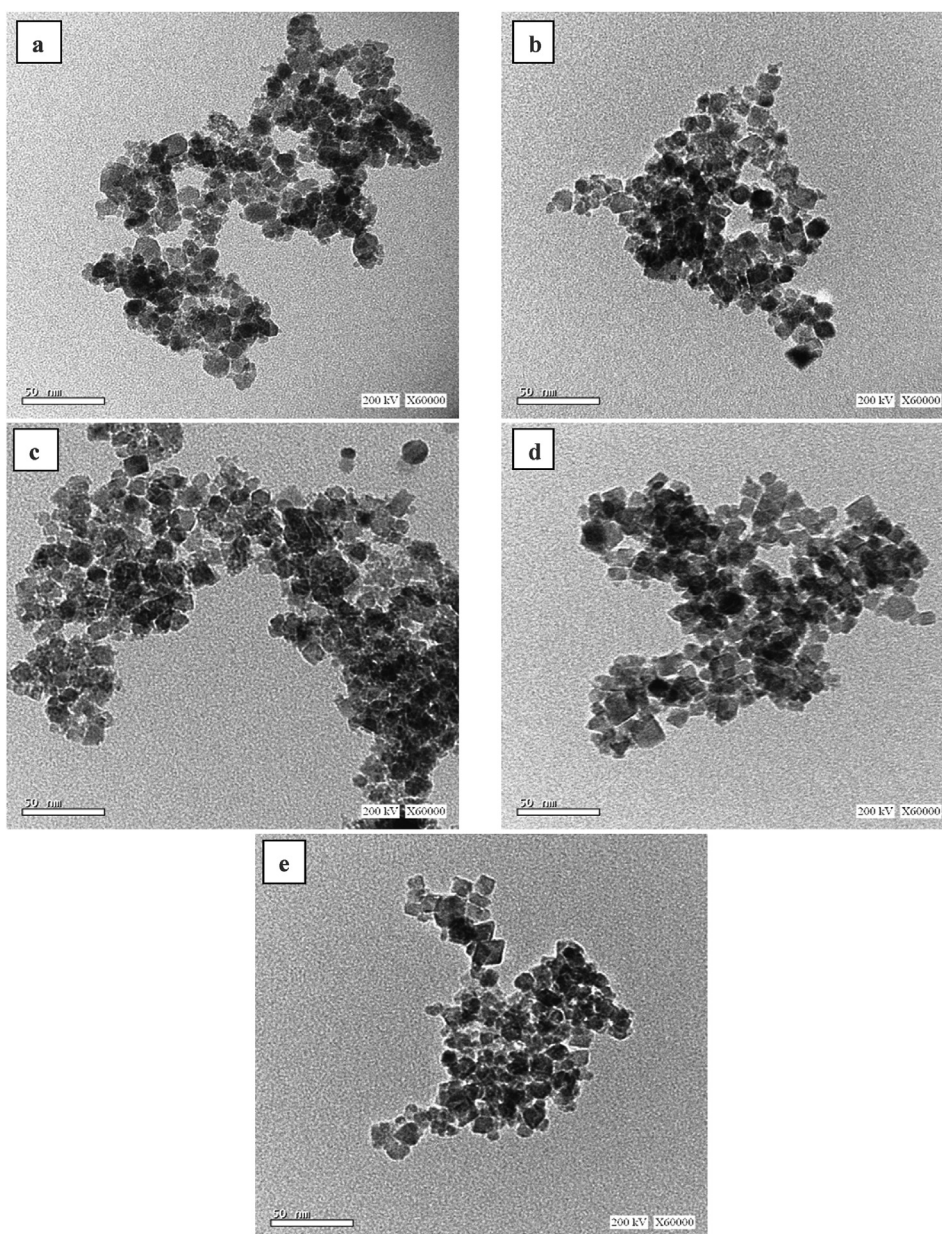
Figure 6. HR-TEM images of ferrite nanofertilizer samples (a) T-100, (b) T-120, (c) T-140, (d) T-160, and (e) T-180.

MAUD software was used to refine the XRD patterns of the five ferrite samples (Figure 2) to quantify the proportion of the produced hematite at each temperature, as shown in Table 1. As the temperature used during the microwave preparation increased, more Fe_2O_3 was produced up to 43% in the sample prepared at 180 °C, whereas the samples prepared at 100 and 120 °C only contained around 1% Fe_2O_3 and 99% ferrite.

3.1.2. Surface area and pore structure analysis

The essential surface and pore features of the synthesized ferrite nanofertilizers were examined using nitrogen gas sorption isotherms as summarized in Table 2. The adsorption-desorption isotherms for all samples exhibited irreversible type IV according to the classification of Brunauer–Deming–Deming–Teller [50] (Figure 3), characteristic for mesoporous structure. Increasing the synthesis temperature from sample T-100 to T-180 caused sintering, as confirmed by the reduction in surface area (Table 2). Evidently, there was a considerable change in the pore structure as the synthesis temperature increased. The adsorption-desorption isotherms of samples T-100, T-120, T-140 showed

H2 type hysteresis [50, 51], pointing out the existence of tightened "ink bottle" pores. This type of pore was implied by Kraemer [52], improved by McBain [53] and others [54, 55], and is composed of a broader body with a constricted inlet "neck". It was observed from the shape of the hysteresis loops of these three samples that the solids had experienced a sort of bottle-neck widening as the synthesis temperature increased, as indicated from the narrowing of the hysteresis loops from sample T-100 to T-140. The further increase in the synthesis temperature, samples T-160 and T-180, caused a drastic change in the porous structure, as confirmed by the presence of H3 hysteresis loops in both samples. This type of hysteresis is characteristic for slit-shaped pores which are produced from particles composing plate-like form as a result of their loosely coherent assembly, proving the occurrence of deformation as a result of the increasing synthesis temperature.

The closure of the hysteresis loops at $p/p° < 0.4$, especially for samples T-100, T-120 and T-140, indicated the presence of some micropores [56], which was confirmed by the BJH pore size distribution curves (Figure 4). Additionally, the broadness of the pore size

Table 3. Effect of ferrite nanofertilizer on plant growth characters of squash plant. (During two successive seasons 2017 and 2018).

Nanoferrite samples	Concentrations	Plant height (cm)		No. of leaves/plant		Leave area/plant (m^2)		Plant weight (g/plant)			
								Fresh		Dry	
		1st	2nd	1st	2nd	1st	2nd	1st	2nd	1st	2nd
T-100	0 ppm	44.2	44.1	17.7	17.3	0.58	0.63	222.6	225.3	27.5	27.1
	10 ppm	51.8	51.3	25.0	25.0	1.15	1.18	378.8	376.7	32.6	32.4
	20 ppm	55.6	55.2	21.3	20.3	1.28	1.28	409.8	405.0	26.9	26.9
	30 ppm	56.0	55.8	19.3	19.7	1.03	1.05	404.6	407.0	35.5	35.3
Mean		**51.9**	**51.6**	**20.8**	**20.6**	**1.01**	**1.04**	**354.0**	**353.5**	**30.6**	**30.4**
T-120	0ppm	44.2	44.1	17.7	17.3	0.58	0.63	222.6	225.3	27.5	27.1
	10 ppm	58.2	58.0	20.7	21.3	1.49	1.44	469.5	463.5	35.4	35.4
	20 ppm	52.8	52.7	23.3	22.7	1.08	1.08	372.1	367.3	34.2	34.1
	30 ppm	47.0	46.3	17.0	18.0	0.80	0.87	251.9	261.3	29.9	30.3
Mean		**50.5**	**50.3**	**19.7**	**19.8**	**0.99**	**1.01**	**329.0**	**329.4**	**31.8**	**31.7**
T-140	0ppm	44.2	44.1	17.7	17.3	0.58	0.63	222.6	225.3	27.5	27.1
	10 ppm	51.1	51.2	25.0	24.3	0.80	0.79	335.6	331.6	24.9	25.2
	20 ppm	55.2	55.4	19.3	20.0	0.93	0.97	345.4	340.6	30.9	30.7
	30 ppm	46.2	46.5	19.0	19.7	0.73	0.74	263.5	271.7	24.0	24.1
Mean		**49.2**	**49.3**	**20.3**	**20.3**	**0.76**	**0.78**	**291.8**	**292.3**	**26.8**	**26.8**
T-160	0ppm	44.2	44.1	17.7	17.3	0.58	0.63	222.6	225.3	27.5	27.1
	10 ppm	55.8	56.0	25.3	25.7	1.29	1.26	417.4	417.4	33.2	33.4
	20 ppm	54.0	53.5	30.3	29.7	0.98	0.99	414.5	406.9	34.7	34.8
	30 ppm	55.0	54.7	18.7	19.3	1.13	1.13	433.8	425.8	40.0	39.8
Mean		**52.3**	**52.1**	**23.0**	**23.0**	**0.99**	**1.00**	**372.1**	**368.8**	**33.8**	**33.8**
T-180	0ppm	44.2	44.1	17.7	17.3	0.58	0.63	222.6	225.3	27.5	27.1
	10 ppm	54.7	54.0	25.0	25.0	0.87	0.86	359.2	361.0	33.3	33.3
	20 ppm	55.3	56.0	33.7	32.7	0.88	0.88	390.5	392.0	35.6	35.6
	30 ppm	58.2	58.9	24.3	25.0	0.99	1.00	344.4	345.9	30.9	30.9
Mean		**53.1**	**53.2**	**25.2**	**25.0**	**0.83**	**0.84**	**329.2**	**331.0**	**31.8**	**31.7**
Average	0ppm	44.2	44.1	17.7	17.3	0.58	0.63	222.6	225.3	27.5	27.1
	10 ppm	54.3	54.1	24.2	24.3	1.12	1.11	392.1	390.0	31.9	31.9
	20 ppm	54.6	54.6	25.6	25.1	1.03	1.04	386.5	382.4	32.4	32.4
	30 ppm	52.5	52.4	19.7	20.3	0.94	0.96	339.7	342.3	32.1	32.1
LSD at 5%	**Effect of temp.**	**2.16**	**1.81**	**2.40**	**1.93**	**N.S.**	**0.19**	**32.11**	**26.76**	**3.39**	**3.31**
	Concentrations	**1.74**	**1.68**	**2.91**	**2.44**	**0.11**	**0.10**	**34.17**	**33.87**	**4.16**	**4.23**
	Interaction	**3.47**	**3.35**	**5.82**	**4.88**	**0.23**	**0.21**	**68.35**	**67.73**	**N.S.**	**N.S.**

N.S = Not Significant ($p < 0.05$).

distribution curves decreased as the synthesis temperature increased, indicating the influence of the temperature in narrowing the pore sizes scattering. This result is in accordance with the decrease in hysteresis loops when the synthesis temperature increased (Figure 3). It is noteworthy that later in section 3.2.1 and section 3.2.2.2, the best sample in terms of squash yield (ton/ha) and total energy resulted from the proximate components of squash fruit (kcal/g) was sample T-160 at optimum concentrations of 10 and 20 ppm, respectively. This sample possessed the narrowest pore radius distribution of all samples as shown in Figure 4, confirming the correlation between pore size distribution and the fertilizing efficiency of the material.

3.1.3. Ferrite morphology and textural analysis

The morphology as well as the particle shape and size of the prepared ferrites were investigated using FE-SEM and HR-TEM as shown in Figures 5 and 6, respectively. All the prepared ferrite particles showed a cubic shape, the crystallinity and regularity of which enhanced as the holding synthesis temperature increased, in agreement with the obtained cubic spinel XRD patterns (Figure 1).

According to FE-SEM images, the particles constituting the material surface became closely packed together as the synthesis temperature increased, eventually forming a large cubic morphological structure (Figure 5e) for sample T-180, resulting in an increment in the intermediate pore size as indicated earlier in the previous section.

Regarding the HR-TEM images, the particle size of the prepared ferrites exhibited a slight increase with the increased microwave holding temperature. The average particle size of the prepared samples for at least 100 particles was estimated from TEM graphs (Figure 6), showing that the average particle size increased with increasing preparation temperature (10.0 ± 2.1, 10.7 ± 2.3, 11.0 ± 2.4, 11.1 ± 1.9, 11.5 ± 2.4 nm for samples T-100, T-120, T-140, T-160, and T-180, respectively), thereby confirming the successful production of nanoparticles via green synthesis without a template.

3.2. Squash planting process

3.2.1. Effect of ferrite nanofertilizer on squash growth and yield

The application of $Mn_{0.5}Zn_{0.5}Fe_2O_4$ NPs as a foliar nanofertilizer significantly improved the growth and fruit characteristics of the squash plant during two successive seasons, 2017 and 2018 (Tables 3 and 4), with these characteristics increasing with concentration and preparation temperature of ferrite nanofertilizer. The highest values of plant height and number of leaves/plant were obtained with sample T-180 (Table 3). But, the leaves area/plant remarkably increased with the preparation temperature of ferrite nanofertilizer (T-100). The highest values of the fresh and dry weight of squash plants were obtained with T-160, reflecting that sample T-160 was enough and suitable to improve the characteristics of growth. However, T-140 nanofertilizer had a

Table 4. Effect of ferrite nanofertilizer on the characters and the yield of squash fruit plant. (During two successive seasons 2017 and 2018).

Nanoferrite samples	Concentrations	Fruit Length (cm)		Fruit Diameter (cm)		Yield kg/plant		Yield t/ha	
		1st	2nd	1st	2nd	1st	2nd	1st	2nd
T-100	0ppm	11.1	11.3	4.7	4.6	0.92	0.90	36.7	36.1
	10 ppm	13.5	13.4	6.0	5.9	1.06	1.07	42.5	42.7
	20 ppm	12.5	12.6	5.7	5.7	1.16	1.16	46.5	46.5
	30 ppm	11.3	11.4	5.2	5.1	0.94	0.97	37.6	38.7
Mean		12.1	12.2	5.4	5.3	1.02	1.03	40.8	41.0
T-120	0ppm	11.1	11.3	4.7	4.6	0.92	0.90	36.7	36.1
	10 ppm	11.7	11.9	5.3	5.2	1.30	1.31	52.1	52.3
	20 ppm	11.3	11.3	5.3	5.2	1.08	1.12	43.1	44.9
	30 ppm	11.3	11.5	5.2	5.1	1.14	1.15	45.7	46.0
Mean		11.4	11.5	5.1	5.0	1.11	1.12	44.4	44.8
T-140	0ppm	11.1	11.3	4.7	4.6	0.92	0.90	36.7	36.1
	10 ppm	12.3	12.5	5.6	5.6	1.19	1.18	47.6	47.1
	20 ppm	13.5	13.6	6.1	6.0	1.20	1.23	48.0	49.3
	30 ppm	13.3	13.4	5.8	5.9	1.31	1.31	52.5	52.5
Mean		12.6	12.7	5.5	5.5	1.15	1.16	46.2	46.3
T-160	0ppm	11.1	11.3	4.7	4.6	0.92	0.90	36.7	36.1
	10 ppm	11.5	11.7	5.2	5.3	1.37	1.38	54.8	55.2
	20 ppm	11.4	11.5	4.6	4.7	1.20	1.22	48.1	48.9
	30 ppm	10.5	10.6	4.2	4.3	1.32	1.32	52.8	52.8
Mean		11.1	11.3	4.7	4.7	1.20	1.21	48.1	48.3
T-180	0ppm	11.1	11.3	4.7	4.6	0.92	0.90	36.7	36.1
	10 ppm	12.2	12.1	5.9	5.9	1.24	1.26	49.6	50.3
	20 ppm	11.9	11.8	5.6	5.7	1.17	1.17	46.8	46.8
	30 ppm	12.1	12.2	5.5	5.6	1.20	1.21	48.1	48.4
Mean		11.8	11.8	5.4	5.5	1.13	1.14	45.3	45.4
Average	0ppm	11.1	11.3	4.7	4.6	0.92	0.90	36.7	36.1
	10 ppm	12.3	12.3	5.6	5.6	1.23	1.24	49.3	49.5
	20 ppm	12.1	12.2	5.5	5.5	1.16	1.18	46.5	47.3
	30 ppm	11.7	11.8	5.2	5.2	1.18	1.19	47.3	47.7
LSD at 5%	Effect of temp.	0.27	0.25	0.19	0.22	0.04	0.04	1.6	1.6
	Concentrations	0.56	0.59	0.31	0.31	0.05	0.06	2.1	2.3
	Interaction	1.13	1.18	0.62	0.62	0.11	0.11	4.3	4.6

considerable effect on the length and diameter of a squash fruit (Table 4). The fruit yield of squash (kg/plant and t/ha) increased with the temperature treatment T-160. These results showed that the growth characteristics were related to the temperature of the preparation of nanoparticles.

Nonetheless, the size of ion also has an impact, as the NPs react with plants to produce several changes in their morphological and physiological properties, based on the properties of NPs. The efficiency of NPs was determined by their chemical structure, size, surface covering, reactivity, and most significantly, the quantity at which they are useful [21]. In addition, the change in the reaction temperature will certainly affect the morphology and structure of the nanomaterials, where the particle morphology is highly dependent on the super-saturation which in turn is dependent upon the solution temperature [57].

Regarding the concentration of ferrite nanofertilizer for foliar application (Tables 3 and 4), the concentration of 20 ppm provided the best values of plant height and number of leaves/plant, which were related to the dry weight of the plant, while the concentration of 10 ppm was more effective on the fresh weight, that was related to length and diameter of fruit, as well as the fruit yield kg/plant and t/ha. Similarly, Zheng et al. [58] illustrated that the concentration of nanoparticles had an effect on processes such as germination and development of the plant. Additionally, Amorós Ortiz-Villajos et al. [33] reported that each element preferentially accumulates in certain parts of the plant, with Cu and Ni in the roots, Mg and Mn in leaves, Ca and Mo in leaves and roots, and K in all parts.

The interaction between the preparation temperature of the ferrite nanofertilizer and the concentration had a significant effect on improving the growth and yield of the squash plant, which were enhanced with increasing preparation temperature as well as their concentration (Tables 3 and 4). The number of leaves per plant improved with T-180 and 20 ppm concentration, with the longest plant length recorded in the plant treated with T-180 at 30 ppm concentration. The highest leaf area per plant and fresh weight per plant was observed in plants treated with T-120 at 10 ppm, with the best fruit length and diameter in plants treated with T-140 at 20 ppm. The fruit yield of squash (kg/plant and t/ha) was enhanced in plants treated with T-160 and 10 ppm concentration.

3.2.2. Effect of ferrite nanofertilizer on proximate components of squash leaves and fruits

3.2.2.1. Effect on squash leaves. The preparation temperature of ferrite nanofertilizer had a notable effect on proximate components of the squash leaves during the seasons 2017 and 2018 (Table 5). Ferrite nanofertilizer prepared at 180 °C (T-180) gave the best values of organic matter and carbohydrate content, which are related to the total energy, while the highest values of protein and ash content were obtained with T-

Table 5. Effect of ferrite nanofertilizer on proximate components of squash leaves. (During two successive seasons 2017–2018).

Nanoferrite samples	Concentrations	Organic matter (%)		Protein (%)		Fiber (%)		Lipids (%)		Carbohydrate (%)		Ash (%)		Total Energy (kcal/g)	
		1st	2nd	1st	2nd	1st	2nd	1st	2nd	1st	2nd	1st	2nd	1st	2nd
T-100	0 ppm	69.5	68.9	21.4	21.3	9.7	9.6	1.7	1.6	36.6	36.3	30.5	31.1	247.7	245.2
	10 ppm	66.7	66.1	21.7	21.5	13.5	13.4	1.0	1.0	30.5	30.2	33.3	33.9	218.1	216.0
	20 ppm	68.1	67.4	20.4	20.3	12.7	12.6	1.4	1.3	33.6	33.3	31.9	32.6	228.3	225.7
	30 ppm	66.5	66.0	23.4	23.2	13.6	13.6	1.4	1.4	28.1	27.8	33.5	34.0	218.7	216.6
Mean		**67.7**	**67.1**	**21.7**	**21.5**	**12.4**	**12.3**	**1.4**	**1.3**	**32.2**	**31.9**	**32.3**	**32.9**	**228.2**	**225.9**
T-120	0ppm	69.5	68.9	21.4	21.3	9.7	9.6	1.7	1.6	36.6	36.3	30.5	31.1	247.7	245.2
	10 ppm	63.8	63.0	22.0	21.6	12.2	12.1	1.2	1.2	28.5	28.1	36.2	37.0	212.7	209.7
	20 ppm	67.1	66.6	23.1	23.1	13.1	13.1	1.7	1.6	29.2	28.8	32.9	33.4	224.5	222.4
	30 ppm	66.2	65.9	20.9	20.7	13.2	13.1	1.3	1.3	30.8	30.7	33.8	34.1	218.0	217.2
Mean		**66.7**	**66.1**	**21.8**	**21.7**	**12.1**	**12.0**	**1.5**	**1.4**	**31.3**	**31.0**	**33.3**	**33.9**	**225.7**	**223.6**
T-140	0ppm	69.5	68.9	21.4	21.3	9.7	9.6	1.7	1.6	36.6	36.3	30.5	31.1	247.7	245.2
	10 ppm	65.4	65.1	22.0	21.9	12.4	12.3	1.7	1.8	29.3	29.2	34.7	34.9	220.5	220.1
	20 ppm	67.7	67.2	22.3	22.2	14.0	13.9	2.9	2.8	28.5	28.3	32.3	32.8	229.5	227.5
	30 ppm	64.7	64.3	24.6	24.4	13.3	13.3	2.0	2.1	24.9	24.6	35.3	35.7	215.4	214.3
Mean		**66.8**	**66.4**	**22.6**	**22.4**	**12.3**	**12.3**	**2.1**	**2.1**	**29.8**	**29.6**	**33.2**	**33.6**	**228.2**	**226.8**
T-160	0ppm	69.5	68.9	21.4	21.3	9.7	9.6	1.7	1.6	36.6	36.3	30.5	31.1	247.7	245.2
	10 ppm	62.5	61.2	21.8	21.6	11.4	11.3	1.5	1.5	27.8	26.8	37.5	38.8	211.7	207.1
	20 ppm	66.1	65.4	24.7	24.5	12.0	11.8	2.0	1.8	27.5	27.3	33.9	34.6	226.5	223.6
	30 ppm	66.3	65.8	24.3	24.2	11.1	11.0	1.8	1.7	29.1	28.9	33.7	34.2	230.3	227.9
Mean		**66.1**	**65.3**	**23.0**	**22.9**	**11.0**	**10.9**	**1.8**	**1.7**	**30.3**	**29.9**	**33.9**	**34.7**	**229.0**	**225.9**
T-180	0ppm	69.5	68.9	21.4	21.3	9.7	9.6	1.7	1.6	36.6	36.3	30.5	31.1	247.7	245.2
	10 ppm	65.5	64.9	22.4	22.3	11.9	11.9	2.2	2.1	29.0	28.6	34.5	35.1	225.4	223.0
	20 ppm	64.4	63.9	22.7	22.6	11.7	11.5	2.0	1.9	28.0	27.8	35.6	36.2	220.7	218.8
	30 ppm	73.0	72.5	23.6	23.4	10.4	10.3	1.9	1.9	37.2	37.0	27.0	27.5	260.0	258.3
Mean		**68.1**	**67.5**	**22.5**	**22.4**	**10.9**	**10.8**	**1.9**	**1.9**	**32.7**	**32.4**	**31.9**	**32.5**	**238.5**	**236.3**
Average	0ppm	69.5	68.9	21.4	21.3	9.7	9.6	1.7	1.6	36.6	36.3	30.5	31.1	247.7	245.2
	10 ppm	64.8	64.1	22.0	21.8	12.3	12.2	1.5	1.5	29.0	28.6	35.2	35.9	217.7	215.2
	20 ppm	66.7	66.1	22.6	22.5	12.7	12.6	2.0	1.9	29.4	29.1	33.3	33.9	225.9	223.6
	30 ppm	67.4	66.9	23.3	23.2	12.3	12.3	1.7	1.7	30.0	29.8	32.7	33.1	228.5	226.9
LSD at 5%	Effect of temp.	0.68	N.S.	0.31	0.31	0.17	0.18	0.10	0.10	0.47	1.54	0.68	N.S.	2.52	6.90
	Concentrations	1.86	1.71	0.82	0.83	0.18	0.19	0.16	0.18	1.02	0.84	1.86	1.71	7.44	6.91
	Interaction	3.72	3.41	1.64	1.65	0.36	0.38	0.32	0.36	2.03	1.68	3.72	3.41	14.89	13.82

160, lipids with T-140 and highest percentage fiber was obtained with T-100 treatment. These results indicate that the preparation temperature of ferrite nanofertilizer had a role in photosynthesis of squash leaves, which may be due to the change in the size and the shape of the prepared nanoferrite (Figures 2 and 3), in agreement with the results reported by Guozhong [57].

In addition, the concentration of ferrite nanofertilizer had a significant effect on proximate components of squash leaves as shown in Table 5, with the maximum percentage of organic matter, carbohydrate and total energy obtained with the highest concentration (30 ppm). The highest protein content was obtained for plants treated with 30 ppm ferrite nanofertilizer, with the highest percentage fiber and lipid content observed in plants treated with 20 ppm concentration. In addition, 10 ppm concentration was more effective on ash percentage, which may be due to the role of the ferrite nanofertilizer in the metabolic processes and penetration of the plant cell.

The interaction between the preparation temperature and concentration of ferrite nanofertilizer also had a significant effect on proximate components of squash leaves (Table 5). The increasing preparation temperature of ferrite nanofertilizer (T-180) with 30 ppm concentration enhanced the organic matter, carbohydrate and total energy (kcal/g). The increase in protein and ash content was greatest in plants treated with 20 and 10 ppm, respectively, T-160. Moreover, the highest percentage lipid and fiber content was observed in plants treated with T-140 at 20 ppm, which may be related to the increased translocation, penetration and accumulation of the nanofertilizer within the plant cell.

3.2.2.2. Effect on squash fruits. The foliar application of the ferrite nanofertilizer had significant effects on the proximate components of the squash fruit (Table 6). T-140 significantly increased organic matter, carbohydrate and total energy (kcal/g), while the highest protein and lipid percentages were obtained in plants treated with T-160. The highest fiber percentage was recorded with plants treated with T-180, and the maximum % ash was obtained in plants treated with T-100. The differences in the proximate component response to nanoparticles produced at different temperatures might be due to the size of nanoparticles and their role in physiological processes in plant cells as stimulating or co-enzymes.

Likewise, the concentration of the ferrite nanofertilizer had an impact on the proximate component of squash fruit (Table 6), indicating that the applied concentrations increased the quality and quantity of squash fruit. The percentage organic matter, protein, carbohydrate and total energy were significantly increased with the concentration of 30 ppm, while lipid was significantly enhanced up to 20 ppm, whereas ash and fiber were most affected by the concentration of 10 ppm.

Regarding the interaction of preparation temperature and concentration (Table 6), the percentage protein and fiber were significantly

Table 6. Effect of ferrite nanofertilizer on proximate components of squash fruits. (During two successive seasons 2017 and 2018).

Nanoferrite samples	Concentrations	Organic matter (%)		Protein (%)		Fiber (%)		Lipids (%)		Carbohydrate (%)		Ash (%)		Total Energy (kcal/g)	
		1st	2nd	1st	2nd	1st	2nd	1st	2nd	1st	2nd	1st	2nd	1st	2nd
T-100	0ppm	76.1	75.7	27.8	27.6	16.0	16.2	1.8	1.9	30.6	30.1	23.9	24.3	249.6	247.3
	10 ppm	70.3	70.4	25.4	25.3	21.3	21.0	1.7	1.8	21.9	22.3	29.7	29.6	204.9	206.4
	20 ppm	72.9	73.2	26.3	26.2	22.3	22.3	2.9	2.7	21.5	22.0	27.1	26.8	216.9	216.9
	30 ppm	71.2	71.7	25.7	25.7	21.4	21.5	2.6	2.5	21.6	22.1	28.8	28.3	212.2	213.3
Mean		72.6	72.7	26.3	26.2	20.2	20.3	2.2	2.2	23.9	24.1	27.4	27.3	220.9	221.0
T-120	0ppm	76.1	75.7	27.8	27.6	16.0	16.2	1.8	1.9	30.6	30.1	23.9	24.3	249.6	247.3
	10 ppm	72.4	72.4	26.6	26.6	20.8	20.7	2.2	2.2	22.9	23.0	27.6	27.6	217.5	217.8
	20 ppm	72.0	71.8	25.1	25.0	20.1	20.1	2.8	2.7	23.9	24.0	28.1	28.2	221.6	220.1
	30 ppm	75.2	74.9	26.1	25.9	19.4	19.1	2.0	2.1	27.8	27.8	24.8	25.1	233.4	233.4
Mean		73.9	73.7	26.4	26.3	19.1	19.0	2.2	2.2	26.3	26.2	26.1	26.3	230.5	229.7
T-140	0ppm	76.1	75.7	27.8	27.6	16.0	16.2	1.8	1.9	30.6	30.1	23.9	24.3	249.6	247.3
	10 ppm	76.2	75.7	28.7	28.6	18.7	18.5	2.5	2.4	26.3	26.2	23.8	24.3	242.2	240.9
	20 ppm	75.4	75.2	26.1	26.3	19.8	19.6	2.2	2.2	27.3	27.2	24.6	24.8	233.3	233.4
	30 ppm	75.6	75.5	28.5	28.5	18.2	18.1	2.2	2.2	26.8	26.8	24.4	24.5	240.8	240.7
Mean		75.8	75.5	27.8	27.7	18.2	18.1	2.2	2.2	27.8	27.6	24.2	24.5	241.5	240.6
T-160	0ppm	76.1	75.7	27.8	27.6	16.0	16.2	1.8	1.9	30.6	30.1	23.9	24.3	249.6	247.3
	10 ppm	70.6	70.1	26.0	25.7	20.1	19.7	3.5	3.3	21.0	21.3	29.4	29.9	219.5	218.0
	20 ppm	76.6	76.3	30.0	29.7	17.7	18.0	3.6	3.4	25.2	25.2	23.4	23.7	253.6	250.3
	30 ppm	76.3	76.4	27.9	28.0	19.5	19.3	2.7	2.8	26.2	26.3	23.8	23.6	240.3	242.0
Mean		74.9	74.6	27.9	27.7	18.3	18.3	2.9	2.8	25.8	25.7	25.1	25.4	240.7	239.4
T-180	0ppm	76.1	75.7	27.8	27.6	16.0	16.2	1.8	1.9	30.6	30.1	23.9	24.3	249.6	247.3
	10 ppm	71.2	71.2	22.8	22.6	24.5	24.5	2.9	2.9	21.0	21.2	28.8	28.8	201.4	201.3
	20 ppm	70.9	70.4	24.1	23.9	24.3	24.1	1.9	2.0	20.6	20.5	29.1	29.6	195.6	195.1
	30 ppm	75.0	74.4	30.4	29.7	18.8	19.1	2.4	2.3	23.4	23.4	25.0	25.6	236.7	232.7
Mean		73.3	72.9	26.3	25.9	20.9	21.0	2.3	2.3	23.9	23.8	26.7	27.1	220.8	219.1
Average	0ppm	76.1	75.7	27.8	27.6	16.0	16.2	1.8	1.9	30.6	30.1	23.9	24.3	249.6	247.3
	10 ppm	72.1	71.9	25.9	25.7	21.1	20.9	2.6	2.5	22.6	22.8	27.9	28.1	217.1	216.9
	20 ppm	73.5	73.4	26.3	26.2	20.9	20.8	2.7	2.6	23.7	23.8	26.5	26.6	224.2	223.2
	30 ppm	74.7	74.6	27.7	27.5	19.4	19.4	2.3	2.4	25.2	25.3	25.3	25.4	232.7	232.4
LSD at 5%	Effect of temp.	0.59	0.36	0.77	0.84	0.23	0.25	0.11	0.20	0.39	0.63	0.59	0.36	1.97	1.66
	Concentrations	0.49	0.56	0.32	0.45	0.13	0.27	0.07	0.14	0.44	0.64	0.49	0.56	2.18	2.60
	Interaction	0.98	1.11	0.65	0.91	0.26	0.53	0.15	0.28	0.89	1.28	0.98	1.11	4.37	5.20

affected in plants treated with T-180 at the concentrations of 30 ppm and 10 ppm, respectively, with the maximum percentage organic matter, lipids and total energy obtained with T-160 at 20 ppm. The percentage ash increased with T-100 at 10 ppm, while carbohydrate improved with T-120 at 30 ppm.

3.2.3. Effect of ferrite nanofertilizer on the mineral contents of squash leaves and fruits

3.2.3.1. Effect on squash leaves.
The prepared ferrite nanofertilizers had significant effects on the mineral content of the leaves during two seasons 2017 and 2018 (Table 7). The mineral content of N and Mn increased most in plants treated with T-160 and T-180, whereas K and Fe were more affected by T-120, while those of P and Zn in leaves were more influenced by T-100. These effects may be due to competition between the shape of NPs and their ability to penetrate the cell wall. Regarding the concentration of NPs, leaf mineral content of N, Zn, Fe and Mn significantly increased with increasing concentration of NPs applied as a foliar fertilizer. The highest concentration 30 ppm applied yielded the highest content of N, Zn, Fe and Mn in leaves, whereas P and K content were greatly affected by 20 and 10 ppm concentration, respectively. The combination of T-160 applied at 20 ppm concentration interaction gave the highest values of N, while T-100 applied at a concentration of 10, 20 and 30 ppm led to an important increase in K, P and Zn leaf content. The highest K content was obtained in plants treated with T-120 at 10 ppm concentration, while Fe and Mn contents

notably increased with 30 ppm of T-120 and T-180, respectively. These results suggest that the increase in the mineral contents of leaves is mostly attributed to the preparation temperature of the ferrite nano-fertilizers and their concentration.

3.2.3.2. Effect on squash fruits.
Data in Table 8 showed that ferrite nanofertilizer also enhanced the mineral content of squash fruits, with T-160 being more effective on N, P, K and Mn content, while Zn content was influenced by the T-100. In this regard, Fe content was remarkably increased by T-140. These results showed that N, P, K and Mn contents of squash fruit were more responsive to the preparation temperature of ferrite nanofertilizer (T-160). Furthermore, the concentration of ferrite nanofertilizer affected the mineral content of squash fruits, with K, Zn and Mn obviously increased by treatment with 10 ppm, while N, P and Fe contents were most affected by 30 ppm, suggesting that the mineral content responses varied according to the ability of penetration and size, thus, the mineral contents decreased with increasing applied ferrite nanofertilizer concentration.

Accordingly, the interaction between the preparation temperature of ferrite nanofertilizers and their concentration showed a significant effect on the mineral content of squash fruits (Table 8). The contents of N and K were more affected by application of T-180 at 30 and 10 ppm, respectively, while P and Mn content were affected by treatment with T-160 at 20 and 30 ppm, respectively. The highest Zn content was obtained by T-100 at 30 ppm, whereas the Fe content increased with treatment with T-140 at 30 ppm.

Table 7. Effect of ferrite nanofertilizer on squash leaves content of the endogenous minerals. (During two successive seasons 2017 and 2018).

Nanoferrite samples	Concentrations	N 1st	N 2nd	P 1st	P 2nd	K 1st	K 2nd	Zn 1st	Zn 2nd	Fe 1st	Fe 2nd	Mn 1st	Mn 2nd
T-100	0	3.43	3.40	0.11	0.10	2.40	2.37	48.0	47.3	120.0	118.3	53.0	53.0
	10 ppm	3.47	3.44	0.31	0.31	4.30	4.23	55.0	57.7	90.0	91.3	26.0	27.0
	20 ppm	3.26	3.24	0.37	0.35	2.76	2.79	103.0	101.0	150.0	153.0	35.0	36.7
	30 ppm	3.74	3.71	0.15	0.16	3.30	3.27	240.0	238.0	290.0	291.7	44.0	45.3
Mean		**3.47**	**3.45**	**0.24**	**0.23**	**3.19**	**3.16**	**111.5**	**111.0**	**162.5**	**163.6**	**39.5**	**40.5**
T-120	0	3.43	3.40	0.11	0.10	2.40	2.37	48.0	47.3	120.0	118.3	53.0	53.0
	10 ppm	3.51	3.45	0.30	0.29	3.80	3.73	25.0	26.7	135.0	133.3	25.0	26.7
	20 ppm	3.70	3.69	0.20	0.19	3.24	3.22	63.0	63.0	150.0	151.7	26.0	28.3
	30 ppm	3.34	3.32	0.13	0.13	3.60	3.57	25.0	26.7	300.0	296.7	53.0	54.3
Mean		**3.49**	**3.47**	**0.19**	**0.18**	**3.26**	**3.22**	**40.3**	**40.9**	**176.3**	**175.0**	**39.3**	**40.6**
T-140	0	3.43	3.40	0.11	0.10	2.40	2.37	48.0	47.3	120.0	118.3	53.0	53.0
	10 ppm	3.52	3.50	0.15	0.16	3.80	3.79	13.0	16.0	150.0	148.3	18.0	20.3
	20 ppm	3.57	3.55	0.14	0.15	3.20	3.22	68.0	68.3	135.0	133.3	44.0	44.7
	30 ppm	3.93	3.90	0.15	0.16	2.00	2.10	18.0	18.0	25.0	26.7	61.0	62.0
Mean		**3.61**	**3.59**	**0.14**	**0.14**	**2.85**	**2.87**	**36.8**	**37.4**	**107.5**	**106.7**	**44.0**	**45.0**
T-160	0	3.43	3.40	0.11	0.10	2.40	2.37	48.0	47.3	120.0	118.3	53.0	53.0
	10 ppm	3.49	3.46	0.22	0.22	3.34	3.32	13.0	13.0	40.0	42.0	26.0	27.0
	20 ppm	3.94	3.91	0.32	0.30	2.00	2.07	33.0	33.0	70.0	70.7	53.0	53.7
	30 ppm	3.89	3.87	0.15	0.16	3.34	3.31	58.0	59.3	100.0	103.0	70.0	72.0
Mean		**3.69**	**3.66**	**0.20**	**0.20**	**2.77**	**2.77**	**38.0**	**38.2**	**82.5**	**83.5**	**50.5**	**51.4**
T-180	0	3.43	3.40	0.11	0.10	2.40	2.37	48.0	47.3	120.0	118.3	53.0	53.0
	10 ppm	3.59	3.57	0.24	0.24	2.00	2.17	93.0	93.7	85.0	86.7	70.0	71.0
	20 ppm	3.63	3.62	0.29	0.28	3.40	3.37	70.0	71.0	80.0	81.7	100.0	101.7
	30 ppm	3.77	3.74	0.22	0.21	3.30	3.28	88.0	86.7	125.0	126.7	118.0	118.7
Mean		**3.61**	**3.58**	**0.22**	**0.21**	**2.78**	**2.80**	**74.8**	**74.7**	**102.5**	**103.3**	**85.3**	**86.1**
Average	0	3.43	3.40	0.11	0.10	2.40	2.37	48.0	47.3	120.0	118.3	53.0	53.0
	10 ppm	3.52	3.48	0.24	0.24	3.45	3.45	39.8	41.4	100.0	100.3	33.0	34.4
	20 ppm	3.62	3.60	0.26	0.25	2.92	2.93	67.4	67.3	117.0	118.1	51.6	53.0
	30 ppm	3.73	3.71	0.16	0.16	3.11	3.11	85.8	85.7	168.0	168.9	69.2	70.5
LSD at 5%	Effect of temp.	0.05	0.05	0.01	0.01	0.05	0.07	2.09	1.59	1.29	3.24	4.13	4.19
	Concentrations	0.13	0.13	0.01	0.01	0.06	0.06	1.99	2.61	1.32	2.24	2.18	2.43
	Interaction	0.26	0.26	0.02	0.02	0.12	0.13	3.97	5.22	2.63	4.48	4.36	4.87

Table 8. Effect of ferrite nanofertilizer on squash fruits content of the endogenous minerals. (During two successive seasons 2017 and 2018).

Nanoferrite samples	Concentrations	N 1st	N 2nd	P 1st	P 2nd	K 1st	K 2nd	Zn 1st	Zn 2nd	Fe 1st	Fe 2nd	Mn 1st	Mn 2nd
T-100	0	4.44	4.41	0.24	0.23	4.20	4.13	62.0	61.0	59.0	60.0	59.0	58.3
	10 ppm	4.07	4.05	0.18	0.17	5.16	5.13	85.0	83.7	63.0	64.7	62.0	61.7
	20 ppm	4.21	4.19	0.24	0.24	4.20	4.27	91.0	90.3	75.0	75.7	61.0	60.3
	30 ppm	4.11	4.11	0.24	0.23	4.87	4.93	99.0	98.0	75.0	75.7	57.3	56.7
Mean		**4.21**	**4.19**	**0.23**	**0.22**	**4.61**	**4.61**	**84.3**	**83.3**	**68.0**	**69.0**	**59.8**	**59.3**
T-120	0	4.44	4.41	0.24	0.23	4.20	4.13	62.0	61.0	59.0	60.0	59.0	58.3
	10 ppm	4.25	4.25	0.34	0.34	4.20	4.13	94.0	94.0	72.0	72.7	59.0	58.7
	20 ppm	4.02	4.00	0.26	0.25	3.60	3.66	83.0	83.7	72.0	73.0	60.0	59.7
	30 ppm	4.17	4.14	0.31	0.30	2.76	2.92	68.0	69.0	65.0	66.0	62.0	62.0
Mean		**4.22**	**4.20**	**0.29**	**0.28**	**3.69**	**3.71**	**76.8**	**76.9**	**67.0**	**67.9**	**60.0**	**59.7**
T-140	0	4.44	4.44	0.24	0.23	4.20	4.13	62.0	61.0	59.0	60.0	59.0	58.3
	10 ppm	4.59	4.57	0.28	0.28	5.76	5.70	98.0	97.0	60.0	60.7	55.0	55.3
	20 ppm	4.18	4.20	0.29	0.28	5.40	5.35	98.0	96.7	74.0	75.0	50.0	51.0
	30 ppm	4.56	4.55	0.28	0.27	3.34	3.42	60.0	61.7	82.0	81.7	41.0	42.7
Mean		**4.44**	**4.43**	**0.27**	**0.27**	**4.68**	**4.65**	**79.5**	**79.1**	**68.8**	**69.3**	**51.3**	**51.8**
T-160	0	4.44	4.41	0.24	0.23	4.20	4.13	62.0	61.0	59.0	60.0	59.0	58.3
	10 ppm	4.16	4.12	0.38	0.38	5.76	5.69	93.0	92.0	64.0	65.0	62.0	61.7
	20 ppm	4.80	4.75	0.57	0.56	6.24	6.11	88.0	88.7	75.0	74.7	60.0	59.3
	30 ppm	4.47	4.47	0.34	0.36	5.50	5.60	62.0	63.0	72.0	72.3	70.0	69.0

Table 8 (*continued*)

Nanoferrite samples	Concentrations	N 1st	N 2nd	P 1st	P 2nd	K 1st	K 2nd	Zn 1st	Zn 2nd	Fe 1st	Fe 2nd	Mn 1st	Mn 2nd
Mean		4.47	4.44	0.38	0.38	5.43	5.38	76.3	76.2	67.5	68.0	62.8	62.1
T-180	0	4.44	4.41	0.24	0.23	4.20	4.13	62.0	61.0	59.0	60.0	59.0	58.3
	10 ppm	3.64	3.61	0.23	0.23	6.70	6.57	83.3	82.0	60.0	61.3	57.0	57.0
	20 ppm	3.85	3.82	0.10	0.10	3.60	3.69	68.0	69.7	64.0	65.3	55.0	54.0
	30 ppm	4.87	4.75	0.42	0.41	5.50	5.56	93.0	92.0	82.0	81.3	41.3	43.3
Mean		4.20	4.15	0.25	0.24	5.00	4.99	76.6	76.2	66.3	67.0	53.1	53.2
Average	0	4.44	3.97	0.24	0.23	4.20	4.13	62.0	61.0	59.0	60.0	59.0	58.3
	10 ppm	4.14	3.67	0.28	0.28	5.52	5.44	90.7	89.7	63.8	64.9	59.0	58.9
	20 ppm	4.21	3.82	0.29	0.29	4.61	4.62	85.6	85.8	72.0	72.7	57.2	56.9
	30 ppm	4.44	3.92	0.32	0.32	4.39	4.49	76.40	76.73	75.2	75.4	54.3	54.7
LSD at 5%	Effect of temp.	0.12	0.13	0.01	0.01	0.05	0.06	1.32	1.37	0.39	0.73	0.95	1.73
	Concentrations	0.05	0.07	0.01	0.01	0.06	0.11	0.94	1.74	0.44	0.89	1.11	1.11
	Interaction	0.10	0.15	0.02	0.02	0.12	0.21	1.87	3.49	0.89	1.79	2.22	2.22

4. Conclusions

Green template-free microwave-assisted hydrothermal synthesis method was successfully applied to prepare manganese zinc ferrites nanoparticles. The synthesized ferrite nanoparticles had a cubic shape, the regularity of which was enhanced as the holding synthesis temperature increased. The synthesized nanoferrites displayed an irreversible type IV adsorption-desorption isotherm, which was attributed to the mesopore capillary condensation effect. In addition, the surface area and broad pore size distribution of these nanoferrites decreased as the synthesis temperature increased, while the average particle size increased. The most effective surface parameter in fertilization efficiency was the pore size distribution. Furthermore, the application of these ferrites as foliar nanofertilizers improved the growth and yield of the squash plant during two successive seasons, with the highest fruit yield of squash per hectare (54.8 & 55.2 t/ha) obtained with nanofertilizer prepared at 160 °C (T-160) and applied at a concentration of 10 ppm. Finally, the results had proven the influence of the synthesis temperature on the physicochemical characteristics of the prepared nanoferrites including surface, pore structure, particles size and shape, and consequently on the plant growth criteria and the yield of squash plants when applied with different concentrations.

Disclosure

Author contribution statement

Ahmed Shebl: Conceived and designed the experiments; Performed the experiments; Analyzed and interpreted the data; Wrote the paper.

Amr A. Hassan, Mohamed S. A. Abd Elwahed: Conceived and designed the experiments; Analyzed and interpreted the data; Wrote the paper.

Dina M. Salama: Performed the experiments; Analyzed and interpreted the data; Wrote the paper.

Mahmoud E. Abd El-Aziz: Analyzed and interpreted the data; Wrote the paper.

Competing interest statement

The authors declare no conflict of interest.

Additional information

No additional information is available for this paper.

References

[1] H. Yan, Q. Chen, J. Liu, Y. Feng, K. Shih, Phosphorus recovery through adsorption by layered double hydroxide nano-composites and transfer into a struvite-like fertilizer, Water Res. 145 (2018) 721–730.

[2] M. Janmohammadi, T. Amanzadeh, N. Sabaghia, S. Dashti, Impact of foliar application of nano micronutrient fertilizers and titanium dioxide nanoparticles on the growth and yield components of barley under supplemental irrigation, Acta Agric. Slov. 107 (2016) 265–276.

[3] R. Liu, R. Lal, Synthetic apatite nanoparticles as a phosphorus fertilizer for soybean (*Glycine max*), Sci. Rep. 4 (2014) 5686.

[4] H. Chhipa, Nanofertilizers and nanopesticides for agriculture, Environ. Chem. Lett. 15 (2017) 15–22.

[5] C.O. Dimkpa, P.S. Bindraban, Correction to nanofertilizers: new products for the industry? J. Agric. Food Chem. 66 (2018), 9158-9158.

[6] S. Mahmoud, D.M. Salama, M. Abd El-Aziz, Effect of chitosan and chitosan nanoparticles on growth, productivity and chemical quality of green snap bean, Biosci. Res. 15 (2018) 4307–4321.

[7] M. Yuvaraj, K. Subramanian, Controlled-release fertilizer of zinc encapsulated by a manganese hollow core shell, Soil Sci. Plant Nutr. 61 (2015) 319–326.

[8] A. Jarosiewicz, M. Tomaszewska, Controlled-Release NPK Fertilizer encapsulated by polymeric membranes, J. Agric. Food Chem. 51 (2003) 413–417.

[9] R. Liu, H. Zhang, R. Lal, Effects of stabilized nanoparticles of copper, zinc, manganese, and iron oxides in low concentrations on lettuce (*Lactuca sativa*) seed germination: nanotoxicants or nanonutrients? *Water*, Air Soil Pollu. 227 (2016) 42.

[10] S. Palchoudhury, K.L. Jungjohann, L. Weerasena, A. Arabshahi, U. Gharge, A. Albattah, J. Miller, K. Patel, R.A. Holler, Enhanced legume root growth with pre-soaking in α-Fe_2O_3 nanoparticle fertilizer, RSC Adv. 8 (2018) 24075–24083.

[11] C. Liu, B. Zou, A.J. Rondinone, Z.J. Zhang, Chemical control of superparamagnetic properties of magnesium and cobalt spinel ferrite nanoparticles through atomic level magnetic couplings, J. Am. Chem. Soc. 122 (2000) 6263–6267.

[12] A.A. Hammad, M.E. Abd El-Aziz, M. Hasanin, S. Kamel, A novel electromagnetic biodegradable nanocomposite based on cellulose, polyaniline, and cobalt ferrite nanoparticles, Carbohydr. Polym. 216 (2019) 54–62.

[13] K. Maaz, A. Mumtaz, S.K. Hasanain, A. Ceylan, Synthesis and magnetic properties of cobalt ferrite ($CoFe_2O_4$) nanoparticles prepared by wet chemical route, J. Magn. Magn Mater. 308 (2007) 289–295.

[14] S.L. Darshane, R.G. Deshmukh, S.S. Suryavanshi, I.S. Mulla, Gas-sensing properties of zinc ferrite nanoparticles synthesized by the molten-salt route, J. Am. Ceram. Soc. 91 (2008) 2724–2726.

[15] S. Rana, A. Gallo, R.S. Srivastava, R.D.K. Misra, On the suitability of nanocrystalline ferrites as a magnetic carrier for drug delivery: functionalization, conjugation and drug release kinetics, Acta Biomater. 3 (2007) 233–242.

[16] K. Kathiravan, G. Vengedesan, S. Singer, B. Steinitz, H.S. Paris, V. Gaba, Adventitious regeneration in vitro occurs across a wide spectrum of squash (*Cucurbita pepo*) genotypes, Plant Cell Tissue Organ Cult. 85 (2006) 285–295.

[17] S. Bandyopadhyay, K. Ghosh, C. Varadachari, Multimicronutrient slow-release fertilizer of zinc, iron, manganese, and copper, Int. J. Chem. Eng. 2014 (2014).

[18] F. Aslani, S. Bagheri, N. Muhd Julkapli, A.S. Juraimi, F.S.G. Hashemi, A. Baghdadi, Effects of engineered nanomaterials on plants growth: an overview, Sci. World J. 2014 (2014) 1–28.

[19] I. Iavicoli, V. Leso, D.H. Beezhold, A.A. Shvedova, Nanotechnology in agriculture: opportunities, toxicological implications, and occupational risks, Toxicol. Appl. Pharmacol. 329 (2017) 96–111.

[20] W. Du, J. Yang, Q. Peng, X. Liang, H. Mao, Comparison study of zinc nanoparticles and zinc sulphate on wheat growth: from toxicity and zinc biofortification, Chemosphere 227 (2019) 109–116.

[21] M.V. Khodakovskaya, K. de Silva, A.S. Biris, E. Dervishi, H. Villagarcia, Carbon nanotubes induce growth enhancement of tobacco cells, ACS Nano 6 (2012) 2128–2135.

[22] S.K. Das, Role of micronutrient in rice cultivation and management strategy in organic agriculture—a reappraisal, Agric. Sci. 5 (2014) 765–769.

[23] A. Sajid, S. Asad, M. Arif, M. Ghazal, A. Imran, M. Sajjad, M. Khan, N. Khan, Enhancement of wheat grain yield and yield components through foliar application of zinc and boron, Sarhad J. Agric. 25 (2009) 15–19.

[24] S. Volkweiss, Sources and methods of application, Micronutri. Agricul. POTAFOS-CNPq: Piracicaba (1991) 391–412.

[25] A. Torun, I. Gültekin, M. Kalayci, A. Yilmaz, S. Eker, I. Cakmak, Effects of zinc fertilization on grain yield and shoot concentrations of zinc, boron, and phosphorus of 25 wheat cultivars grown on a zinc-deficient and boron-toxic soil, J. Plant Nutr. 24 (2001) 1817–1829.

[26] N. Fageria, V. Baligar, R. Clark, Micronutrients in crop production, in: Advances in Agronomy, Elsevier, 2002, pp. 185–268.

[27] D.M. Salama, S.A. Osman, M.E. Abd El-Aziz, M.S.A. Abd Elwahed, E.A. Shaaban, Effect of zinc oxide nanoparticles on the growth, genomic DNA, production and the quality of common dry bean (*Phaseolus vulgaris*), Biocatal. Agricul. Biotechnol. 18 (2019) 101083.

[28] B.J. Alloway, Zinc in Soils and Crop Nutrition, International Zinc Association Brussels, Belgium, 2008.

[29] K. Karthika, I. Rashmi, M. Parvathi, Biological functions, uptake and transport of essential nutrients in relation to plant growth, in: Plant Nutrients and Abiotic Stress Tolerance, Springer, 2018, pp. 1–49.

[30] S.B. Schmidt, P.E. Jensen, S. Husted, Manganese deficiency in plants: the impact on photosystem II, Trends Plant Sci. 21 (2016) 622–632.

[31] G.R. Rout, S. Sahoo, Role of iron in plant growth and metabolism, Rev. Agri. Sci. 3 (2015) 1–24.

[32] R. Sheykhbaglou, M. Sedghi, B. Fathi-Achachlouie, The effect of ferrous nano-oxide particles on physiological traits and nutritional compounds of soybean (*Glycine max L.*) seed, An Acad. Bras Ciências 90 (2018) 485–494.

[33] J.A. Amorós Ortiz-Villajos, F.J. Garcia Navarro, C.J. Sánchez Jiménez, C. Pérez de los Reyes, R. García Moreno, R. Jiménez Ballesta, Trace elements distribution in red soils under semiarid Mediterranean environment, Int. J. Geosci. 2 (2011) 84–97.

[34] S. Jayasubramaniyan, S. Balasundari, P.A. Rayjada, N. Satyanarayana, P. Muralidharan, Microwave hydrothermal synthesis of α-MnMoO₄ nanorods for high electrochemical performance supercapacitors, RSC Adv. 8 (2018) 22559–22568.

[35] L. Zhenyu, X. Guangliang, Z. Yalin, Microwave assisted low temperature synthesis of MnZn ferrite nanoparticles, Nanoscale Res. Lett. 2 (2007) 40–43.

[36] A. Shebl, A.A. Hassan, D.M. Salama, M.E. Abd El-Aziz, M.S. Abd Elwahed, Green synthesis of nanofertilizers and their application as a foliar for Cucurbita pepo L, J. Nanomater. 2019 (2019) 11.

[37] R. Chintaparty, B. Palagiri, R.R. Nagireddy, W. Madhuri, Effect of pH on structural, optical and dielectric properties of nano-zirconium oxide prepared by hydrothermal method, Mater. Lett. 161 (2015) 770–773.

[38] L. Kashinath, K. Namratha, K. Byrappa, Microwave assisted facile hydrothermal synthesis and characterization of zinc oxide flower grown on graphene oxide sheets for enhanced photodegradation of dyes, Appl. Surf. Sci. 357 (2015) 1849–1856.

[39] C. Blanco-Andujar, D. Ortega, P. Southern, Q. Pankhurst, N. Thanh, High performance multi-core iron oxide nanoparticles for magnetic hyperthermia: microwave synthesis, and the role of core-to-core interactions, Nanoscale 7 (2015) 1768–1775.

[40] H. Zhu, X. Wang, Y. Li, Z. Wang, F. Yang, X. Yang, Microwave synthesis of fluorescent carbon nanoparticles with electrochemiluminescence properties, Chem. Commun. 34 (2009) 5118–5120.

[41] D. Nassef, H. El-aref, Effect of foliar spray with iaa and GA3 on production and protein synthesis of two summer squash hybrid cultivars, Egypt. J. Hortic. 45 (2018) 121–143.

[42] P. Feldsine, C. Abeyta, W.H. Andrews, AOAC International methods committee guidelines for validation of qualitative and quantitative food microbiological official methods of analysis, J. AOAC Int. 85 (2002) 1187–1200.

[43] M.E. Abd El-Aziz, S.M.M. Morsi, D.M. Salama, M.S. Abdel-Aziz, M.S. Abd Elwahed, E.A. Shaaban, A.M. Youssef, Preparation and characterization of chitosan/ polyacrylic acid/copper nanocomposites and their impact on onion production, Int. J. Biol. Macromol. 123 (2019) 856–865.

[44] T.U. Nwabueze, Nitrogen solubility index and amino acid profile of extruded African breadfruit (*T. africana*) blends. *Niger*, Food J 25 (2007) 23–35.

[45] T. Hao, Q. Zhu, M. Zeng, J. Shen, X. Shi, X. Liu, F. Zhang, W. de Vries, Quantification of the contribution of nitrogen fertilization and crop harvesting to soil acidification in a wheat-maize double cropping system, Plant Soil 434 (2019) 167–184.

[46] T. Kobata, M. Koç, C. Barutçular, K.-i. Tanno, M. Inagaki, Harvest index is a critical factor influencing the grain yield of diverse wheat species under rain-fed conditions in the Mediterranean zone of southeastern Turkey and northern Syria, Plant Prod. Sci. 21 (2018) 71–82.

[47] A. Iqbal, K. Ali, Formulating the effects of concentration (x) and calcination temperature on the synthesis of $Mn_{1-x}Zn_xFe_2O_4$ by using response surface methodology, J. As. Ceram. Soc. 1 (2013) 333–338.

[48] O.M. Lemine, Microstructural characterisation of α-Fe₂O₃ nanoparticles using, XRD line profiles analysis, FE-SEM and FT-IR, Superlattice. Microst. 45 (2009) 576–582.

[49] Y. El Mendili, J.-F. o. Bardeau, N. Randrianantoandro, F. Grasset, J.-M. Greneche, Insights into the mechanism related to the phase transition from γ-Fe₂O₃ to α-Fe₂O₃ nanoparticles induced by thermal treatment and laser irradiation, J. Phys. Chem. C 116 (2012) 23785–23792.

[50] S.J. Gregg, K.S.W. Sing, R. Haul, Adsorption, surface area and porosity. 2. Auflage, Academic Press, London, Ber. Bunsen Ges. Phys. Chem. 86 (1982), 957-957.

[51] P.T. Tanev, L.T. Vlaev, An attempt at a more precise evaluation of the approach to mesopore size distribution calculations depending on the degree of pore blocking, J. Colloid Interface Sci. 160 (1993) 110–116.

[52] E.O. Kraemer, others, A Treatise on Physical Chemistry; Taylor, D. Van Nostrand Co., New York, 1931.

[53] J.W. McBain, An explanation of hysteresis in the hydration and dehydration of gels, J. Am. Chem. Soc. 57 (1935) 699–700.

[54] M. Thommes, Physical adsorption characterization of nanoporous materials, Chem. Ing. Tech. 82 (2010) 1059–1073.

[55] P.I. Ravikovitch, A.V. Neimark, Experimental confirmation of different mechanisms of evaporation from ink-bottle type Pores: equilibrium, pore blocking, and cavitation, Langmuir 18 (2002) 9830–9837.

[56] G.M. El Shafei, N.A. Moussa, Z.A. Omran, Titania-induced changes of silica texture upon moderate heating, Powder Technol. 107 (2000) 118–122.

[57] C. Guozhong, Nanostructures and Nanomaterials: Synthesis, Properties and Applications, World scientific, 2004.

[58] L. Zheng, F. Hong, S. Lu, C. Liu, Effect of nano-TiO₂ on strength of naturally aged seeds and growth of spinach, Biol. Trace Elem. Res. 104 (2005) 83–91.